

Impact of stimulus duration on motor unit thresholds and alternation in compound muscle action potential scans



Boudewijn T.H.M. Sleutjes^{a,*}, Janna Ruisch^b, Thijs E. Nassi^b, Jan R. Buitenweg^b, Leonard J. van Schelven^c, Leonard H. van den Berg^a, Hessel Franssen^{a,1}, H. Stephan Goedee^{a,1}

^a Department of Neurology, Brain Centre Utrecht, University Medical Centre Utrecht, Utrecht, the Netherlands

^b Biomedical Signals and Systems, Technical Medical Centre, University of Twente, Enschede, the Netherlands

^c Department of Medical Technology and Clinical Physics, University Medical Center Utrecht, the Netherlands

ARTICLE INFO

Article history:

Accepted 26 October 2020

Available online 2 December 2020

Keywords:

Surface-electromyography
Compound muscle action potential scan
Motor units
Threshold variability
Activation thresholds
Alternation

HIGHLIGHTS

- The level of motor unit alternation in compound muscle action potential scans alters markedly by varying the stimulus duration.
- The threshold variability of individual motor units remains unaffected by varying the stimulus duration.
- Implementation of compound muscle action potential scans in a clinical setting requires standardization of stimulation settings.

ABSTRACT

Objective: To investigate the impact of stimulus duration on motor unit (MU) thresholds and alternation within compound muscle action potential (CMAP) scans.

Methods: The stimulus duration (0.1, 0.2, 0.6, and 1.0 ms) in thenar CMAP scans and individual MUs of 14 healthy subjects was systematically varied. We quantified variability of individual MU's thresholds by relative spread (RS), MU thresholds by stimulus currents required to elicit target CMAPs of 5% (S5), 50% (S50) and 95% (S95) of the maximum CMAP, and relative range (RR) by $100 \times [S95 - S5] / S50$. We further assessed the strength-duration time constant (SDTC). Experimental observations were subsequently simulated to quantify alternation.

Results: RS, unaffected by stimulus duration, was 1.65% averaged over all recordings. RR increased for longer stimulus duration (11.4% per ms, $p < 0.001$). SDTC shortened with higher target CMAPs (0.007 ms per 10% CMAP, $p < 0.001$). Experiments and simulations supported that this may underlie the increased RR. A short compared to long stimulus duration recruited relative more MUs at S50 (more alternation) than at the tails (less alternation).

Conclusions: The stimulus duration significantly affects MU threshold distribution and alternation within CMAP scans.

Significance: Stimulation settings can be further optimized and their standardization is preferred when using CMAP scans for monitoring neuromuscular diseases.

© 2020 International Federation of Clinical Neurophysiology. Published by Elsevier B.V. This is an open access article under the CC BY license (<http://creativecommons.org/licenses/by/4.0/>).

1. Introduction

The compound muscle action potential (CMAP) scan is an emerging practical neurophysiological tool, that provides clinically

relevant characteristics on number of motor unit (MUs), MU sizes and motor axon excitability (Drenthen et al., 2008, 2013; Garg et al., 2017; Henderson et al., 2006, 2007, 2009; Jacobsen et al., 2017; Maathuis et al., 2013; Sleutjes et al., 2014). Previous studies have shown its potential as a sensitive bedside tool to evaluate disease severity and progression in several neuromuscular disorders, such as amyotrophic lateral sclerosis (ALS), spinal muscular atrophy (SMA), and peripheral neuropathies (Baumann et al., 2012a, 2012b; Drenthen et al., 2013, 2014; Garg et al., 2017; Henderson

* Corresponding author at: Department of Neurology, F02.230, University Medical Centre Utrecht, P.O. Box 855000, 3508 GA Utrecht, the Netherlands.

E-mail address: b.sleutjes@umcutrecht.nl (B.T.H.M. Sleutjes).

¹ Authors contributed equally.

et al., 2007; Jacobsen et al., 2019; Maathuis et al., 2013; Sleutjes et al., 2020; van der Heyden et al., 2013). The recent advance of more sophisticated treatment strategies in neuromuscular disorders, such as gene targeted therapies, has resulted in exponential increase in costs and demand reliable and efficient tools to monitor therapeutic efficacy. A recent study showed that early changes in patients that received intramuscular stem cell treatment were detected with the CMAP scan but not with other techniques, indicating that the CMAP scan may be more suitable to evaluate treatment efficacy (Geijo-Barrientos et al., 2020). The CMAP scan is further well-tolerated showing high reproducibility and is less labour intensive than various other motor unit number estimate (MUNE) methods (Bostock, 2016; Jacobsen et al., 2017; Maathuis et al., 2011).

The CMAP scan is effectively a stimulus–response curve that can be recorded with routine surface electromyography (EMG) electrodes, using gradually increasing transcutaneous nerve stimulus currents that yield successive activation of all functional MUs. Besides pathophysiological factors, also technical factors, such as the stimulation settings significantly impact the CMAP scan pattern (Maathuis et al., 2012) and, consequently, affect the quantitative measures derived from it (Maathuis et al., 2012; Zong et al., 2020). These settings involve number of stimuli, recording direction, type of sampling, stimulus frequency and duration. The impact of these settings should be well understood to adequately standardize across multiple centers and to determine reference values. Further insights into these factors may also improve the reproducibility and increase the sensitivity of the CMAP scan when applied optimally.

The variation between CMAP scans are mostly dominated by the number of MUs, their sizes, and activation threshold characteristics (Blok et al., 2007; Bostock, 2016; Sleutjes et al., 2014). As the number of MUs and their sizes remain unaffected by the applied stimulation settings, it is their MU activation thresholds, and particularly, the interaction between the distribution of MU activation thresholds and the threshold variability of individual MUs that mark the CMAP scan pattern. Due to this interaction, the activity of multiple MUs may overlap at a fixed stimulus current, also known as alternation (Milner-Brown and Brown, 1976). Mitigating alternation underlies the developments of various MUNE methods to improve on the original incremental approach (de Carvalho et al., 2018; Gooch et al., 2014; McComas et al., 1971).

The stimulus duration mainly affects MU activation thresholds according to their strength-duration properties (Bostock, 1983). In contrast, animal and computational studies have suggested that the threshold variability quantified as relative spread (RS) remains constant over a range of stimulus durations (Lecar and Nossal, 1971a,b; Verveen, 1960). There is, however, limited experimental observations in human subjects on threshold variability (Hales et al., 2004), likely due to the difficulty of identifying isolated responses from single MUs reliably. With the design of a novel approach, we have partly overcome the latter by integrating high-density surface-EMG with excitability testing (Sleutjes et al., 2018). This allows us to assess the yet unexplored impact of stimulus duration on the interaction between the distribution of MU activation thresholds and the threshold variability of individual MUs in human subjects, and, consequently, alternation in CMAP scans. We hypothesize that the level of alternation is significantly affected by stimulus duration.

To evaluate our hypothesis, we performed a systematic study in healthy controls using high-density surface-EMG and single-channel surface-EMG recordings, to assess threshold variability of individual MUs and the distribution of MU activation thresholds in the CMAP scan with varying stimulus durations. Also with the aid of computer simulations, we determined in detail the impact of stimulus duration on alternation.

2. Methods

2.1. Subjects

We recruited 14 healthy volunteers (8 males and 6 females; mean age: 29 years, range: 23–50 years) who underwent individual MU and CMAP scan recordings. Exclusion criteria were signs or symptoms of any neurological disease that could affect functioning of MUs. All subjects gave informed consent for the experiments. The study was in accordance with the principles of the Declaration of Helsinki and approved by the local ethical committee.

2.2. Individual MU potential recordings using high-density surface-EMG

We applied a recently designed setup, where we have integrated high-density surface-EMG with excitability testing to reliably identify individual MU potentials (MUPs) (Sleutjes et al., 2018). As such we can make use of the unique spatiotemporal profiles of individual MUs for their reliable identification using a specifically designed user interface that provided visual feedback during the experiments. The high-density grid consists of a 9x14 array of densely spaced electrodes attached to the skin over the thenar muscle group. From the 126 channels a single-channel surface-EMG signal was fed into the excitability software (Qtrac-S, TRONDNF, version 19/06/2015, Institute of Neurology, Queen Square, London, UK) for tracking the threshold of single MUPs. Similar to our previously described protocol, the optimal channel was qualitatively judged by selecting a channel with the largest surface-EMG signal to improve signal-to-noise ratio and minimal interference with other individual MUPs (Sleutjes et al., 2018).

We sampled one individual MUP in each healthy volunteer, which we obtained from the thenar muscles with standardized stimulation of the median nerve at the wrist based on low stimulus currents using non-polarizable surface electrodes (Red dot, 3 M electrodes Health care). The stimulus sites along the wrist were slightly varied to determine the optimal location for isolating individual MUP responses. A similar location of the cathode as during CMAP scan recordings was the preferred position. The anode was positioned approximately 10 cm proximally, on the radial side of the forearm. A target amplitude was set slightly lower than the measured baseline to negative peak MUP amplitude to define an individual MUP response being present or absent. Subsequently, the excitability program was used to automatically determine the current at which approximately 50% of the stimuli resulted in a MUP response, the definition of the activation threshold in classical electrophysiology.

Stimuli were then delivered uniformly over a stimulus current range to enable reliable tracking of the activation threshold of individual MUPs. From the percentage of stimuli that resulted in a MUP response over this stimulus current range, a cumulative Gaussian probability function was fitted to obtain the mean activation threshold (μ) and standard deviation of the activation threshold (σ). Similar to the findings by Hales et al. (Hales et al., 2004) the threshold variability was quantified by dividing σ by μ , also known as the relative spread (RS).

The stimulus current range needs to be set such that it captures most of the alternating behavior of the MUP responses (“all-or-none” responses of an individual MU) to adequately fit these two parameters (μ , σ). Given the definition of RS and the equivalence to a normal distribution, a stimulus current range set at $\pm 1 \cdot \sigma$ captures approximately 68%, $\pm 2 \cdot \sigma$ approximately 95%, and $\pm 3 \cdot \sigma > 99\%$ of the alternating behavior. The additional information on alternation with a range of $\pm 4 \cdot \sigma$ or higher is therefore negligible. A range

set too narrow (e.g. $\leq 1 \cdot \sigma$) misses a lot of relevant alternating behavior, while a range set to too wide (e.g. $> 3 \cdot \sigma$) makes stimuli superfluous at the boundaries of this range (i.e. mostly absence of alternation, because MUs will either always show a response or never show a response). We therefore used a relative broad stimulus current range of $\pm 3 \cdot \sigma$ with a conservative assumed RS of 2% (Bostock, 2016). So, for example, for a mean activation threshold of 10 mA (μ), the stimulus current range was set at 9.4 mA–10.6 mA (± 0.6 mA $\rightarrow \pm 6\%$ of 10 mA $\rightarrow \pm 3 \cdot RS \cdot \mu \rightarrow \pm 3 \cdot \sigma$). The stimuli were then randomly applied between 9.4 mA–10.6 mA resulting in a uniform distribution of stimulus intensities over this particular range.

In total 600 stimuli were delivered at 1 Hz for each of the four stimulus durations of 0.1 ms, 0.2 ms, 0.6 ms and 1.0 ms. We occasionally reversed the order of stimulus durations between subjects. To further address slow fluctuations of the activation threshold during the recordings, a moving window of 50 stimuli was applied shifted by a single stimulus at the time in the RS analysis. The RS and strength-duration time constant (SDTC) using Weiss's law (Bostock, 1983; Mogyoros et al., 1996) was determined within every individual MU. For data analyses, the individual MUP responses and applied stimulus currents were imported and further processed into Matlab (R2014b: The MathWorks, Natick, Massachusetts, USA).

2.3. CMAP scan recordings using single-channel surface-EMG

The CMAP scan recordings were performed with the MScan program, which is part of the excitability software (Qtrac-S, TRONDNF, version 19/06/2015, Institute of Neurology, Queen Square, London, UK). We obtained baseline to negative peak CMAP amplitude responses from the thenar muscles in the left arm by transcutaneous stimulation of the median nerve. The single active recording electrode was positioned over the muscle belly and the reference electrode was placed at the interphalangeal joint of the first digit. We used a standardized distance between stimulus site (wrist) and the active recording electrode of 7 cm proximal. First, we determined, the stimulus current (S100) required to elicit the maximum CMAP amplitude. Subsequently, the program automatically delivered stimuli of slowly exponentially decreasing stimulus currents at 2 Hz. The program was stopped at the stimulus current where the lowest-threshold MU became inactive (S0), which resulted approximately in 500–700 stimuli per subject. As every MU has a specific activation threshold, the stimulus current range from S0 to S100 reflects the interval in which all of the MUs innervating the muscle become gradually active.

The procedures described above were repeated using stimulus durations of 0.1 ms, 0.2 ms, 0.6 ms and 1.0 ms to determine the impact of stimulus duration on the CMAP scan pattern. Similarly, the order of stimulus durations was occasionally reversed between subjects for the CMAP scan. To provide an indication on the distribution of MU activation threshold from low-to-high threshold MUs in the CMAP scan, stimulus currents to elicit a target CMAP at 5% (S5), 50% (S50), and 95% (S95) of the maximum CMAP were determined together with the relative range defined by $100 \cdot [S95 - S5] / S50$. Additionally, we determined a predefined set of relative thresholds across the CMAP scan by $100 \cdot S5 / S50$, $100 \cdot S10 / S50$, until $100 \cdot S95 / S50$ in steps of 5%. These relative thresholds describe a curve which is smaller than 100% below S50, larger than 100% above S50, and which intersect 100% in the middle ($100 \cdot S50 / S50$). We further determined SDTC within the CMAP scan from target CMAPs at 10% to 90% in steps of 10%. Also, we measured the skin temperature before and after the recordings at the stimulation site using an infrared thermometer (KM814, Comark Limited, Stevenage, UK). For data analyses, the CMAP scan data was

imported and further processed into Matlab (R2014b: The MathWorks, Natick, Massachusetts, USA).

2.4. Simulating alternation in the CMAP scan

We modified a previously developed computer model to generate simulated CMAP scans (Blok et al., 2007; Sleutjes et al., 2014). This model includes parameters that are considered to mainly underlie the variation between CMAP scans, and includes the number of MUs, their sizes and activation threshold characteristics (Blok et al., 2007; Bostock, 2016; Sleutjes et al., 2014). To simplify our simulations, we assumed a fixed set of 200 MUs, which is equivalent to MU estimates in the thenar muscles of healthy subjects (Aggarwal, 2012; Gooch et al., 2014). Furthermore, the simulations involved MU activation thresholds only, irrespective of their sizes. The distribution of MU activation thresholds and the threshold variability of individual MUs were set such that they matched our experimental observations. In short, an activation threshold corresponds to where MUs have a 50% probability of being activate (μ). To simulate threshold variability, we defined a threshold range that reflects the range where individual MUs are probabilistically active. The threshold range was set at twice the RS. Overlapping threshold ranges between MUs were added together to determine the number of probabilistically active MUs. The number of combinations of alternating MUs increases exponentially, 2^n , where n reflects the number of MUs with overlapping threshold ranges. A large n results in a large variability of CMAPs at a fixed stimulus current, while a small n , increases the likelihood of observing the all-or-none responses of individual MUs. Simulating the distribution of MU activation thresholds and threshold variability of individual MUs by threshold ranges gives the possibility to estimate the level of alternation across the entire CMAP scan. Finally, we also assessed and verified the impact of stimulus duration on the level of alternation.

2.5. Statistical analysis

Statistical tests were performed in Matlab (R2014b: The MathWorks, Natick, Massachusetts, USA). We used a linear regression model to evaluate the relationship between the CMAP scan and individual MU outcomes. To determine whether RS and RR were linearly related to the four stimulus durations, we deployed a linear mixed-effects model with RR and RS as response, the within-subject (individual MU or CMAP scan recordings) as random intercept and slope, and the stimulus duration as fixed effects. Similarly, for SDTC, a linear mixed effects model was used with SDTC as response, the within-subject CMAP scan recordings as random intercept and slope, and the target CMAPs as fixed effects. A p -value of < 0.05 was considered statistically significant.

3. Results

3.1. Threshold variability of individual MUs and stimulus currents to elicit CMAP scans

Fig. 1 shows a representative example of individual MUP responses (Fig. 1A) and a CMAP scan (Fig. 1B) recorded within one subject using a stimulus duration of 1.0 ms. To determine the relative spread (RS) and relative range (RR), we normalized the individual MUP and CMAP responses (Fig. 1C and D). The individual MU had a mean activation threshold, μ , of 2.285 mA and standard deviation, σ , of 0.041 mA, resulting in an RS of 1.79% (Fig. 1C). The stimulus currents required to elicit a target CMAP of 5%, 50%, and 95% of the maximum CMAP were 2.577 mA, 3.446 mA, and 4.373 mA respectively, which resulted in a RR of

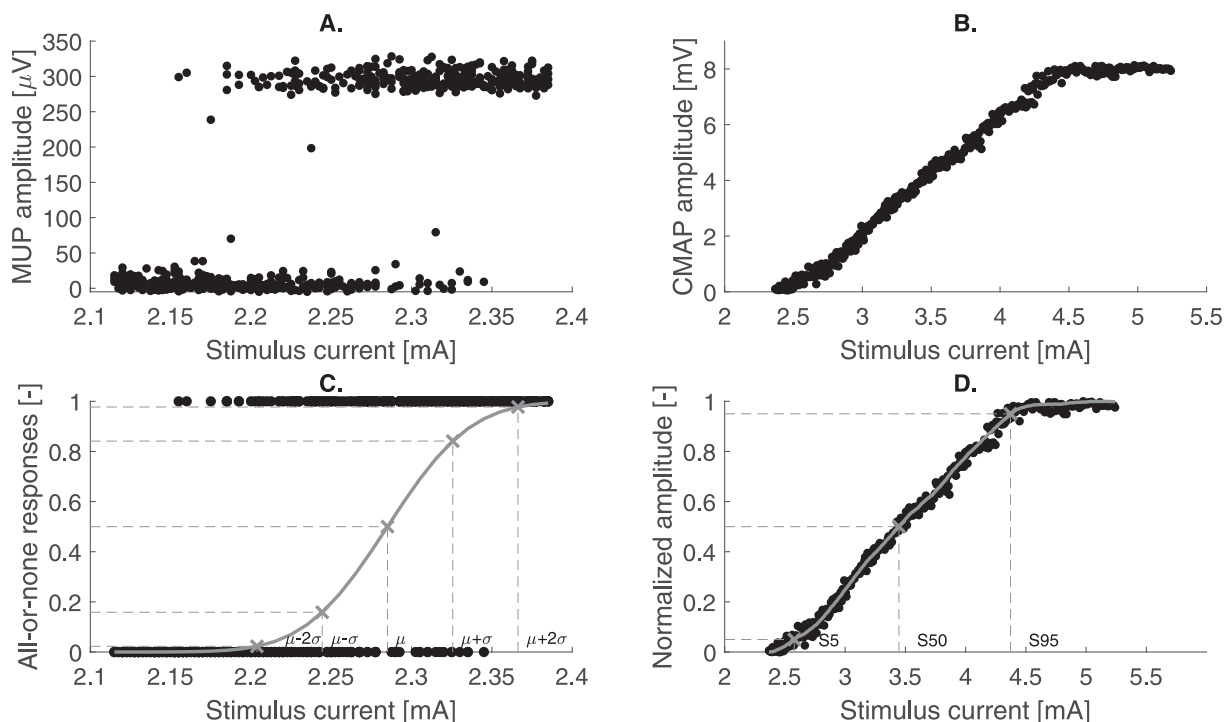


Fig. 1. Example of individual motor unit potentials responses and compound muscle action potential scan responses. Individual motor unit potential (MUP) responses with (A) absolute amplitudes and normalized all-or-none responses (C) with the fitted mean activation threshold, μ , and standard deviation, σ (in gray). These values correspond with $\mu = 2.285$ mA and $\sigma = 0.041$ mA resulting in a relative spread of 1.79%. The compound muscle action potential (CMAP) scan with (B) absolute amplitudes and normalized amplitudes (D) together with the calculated S5 (2.577 mA), S50 (3.446 mA), and S95 (4.373 mA) (in gray). The values correspond with a relative range of 52.1%. The individual MUP responses and the CMAP scan were obtained in the same subject with a 1.0 ms stimulus duration. MUP = motor unit potential, CMAP = compound muscle action potential.

52.1% (Fig. 1D). Similar procedures were applied for all healthy subjects and four stimulus durations. The skin temperature was $30.3 \text{ }^\circ\text{C} \pm 1.8 \text{ }^\circ\text{C}$ (mean \pm SD) during the CMAP scan recordings and $30.6 \text{ }^\circ\text{C} \pm 2.0 \text{ }^\circ\text{C}$ (mean \pm SD) during the individual MU recordings. Table 1 shows the impact of the stimulus duration on threshold variability of individual MUs and the distribution of MU activation thresholds in the 14 healthy subjects.

3.2. Impact of stimulus duration on threshold variability and distribution of thresholds

Fig. 2 shows the relation between stimulus duration and RS and RR. We found that RS had considerable variability across the applied range of stimulus durations, without a clear relation (0.08% per ms, $p = 0.47$; 95% CI $-0.13\% - 0.29\%$). Consequently, we therefore averaged RS across all the 56 recordings that included the 14 individual MUs (one individual MU per healthy volunteer) which were recorded each 4 times (4 different stimulus durations) resulting in an RS of $1.65 \pm 0.43\%$ (mean \pm SD, $n = 56$). In contrast, RR showed a significant increasing pattern towards longer stimulus durations with a mean of 11.4% per ms ($p < 0.001$; 95% CI 7.9%–14.9%).

3.3. Strength-duration time constant in individual MUs and for low-to-high target CMAPs

The mean SDTC in the individual MUs was 0.29 ± 0.06 ms (mean \pm SD, $n = 14$, Fig. 3A). Fig. 3B shows the SDTC across target CMAPs, where black lines correspond to individual subjects. Although moderate variation of SDTC was seen within individual subjects across the different target CMAPs, we found an inverse relation between SDTC and increasing target CMAP values with a

mean SDTC shortening of 0.007 ms per target CMAP of 10% ($p = 0.001$, 95% CI 0.003–0.01; Fig. 3B). For individual MUP responses, the stimulus site slightly varied, because isolated MUP responses were not always clearly present at the stimulation site for CMAP scans. The SDTC of individual MUs was therefore likely smaller than the SDTC at a target CMAP of 10% ($p = 0.003$). At a target CMAP of 90% the difference was not significant ($p = 0.08$). We found no relation between RS and SDTC within individual MUs ($r = 0.20$, $p = 0.45$).

3.4. Simulating the distribution of activation thresholds and alternation in CMAP scans

We implemented our experimental observations into the simulations, to determine alternation in CMAP scans, by assigning normal distributed MU activation thresholds to a fixed pool of 200 MUs with a mean of 5.0 mA (S50 at 1.0 ms, Table 1). We used the RR of 48.7% (RR at 1.0 ms, Table 1) to define the standard deviation. Assuming that the numerator of RR, S95–S5, reflects an approximation of 4 standard deviations of a normal distribution (see Fig. 1C), the standard deviation was set at 12.2% (≈ 0.61 mA). As RS was not significantly affected by stimulus duration, we randomly assigned individual MUs a normal distributed RS of $1.65 \pm 0.43\%$. To determine the level of alternation, we simulated the number of probabilistically active MUs by setting a threshold range at twice the RS surrounding the MU activation threshold (e.g. with $\mu = 5$ mA, the threshold range 5.0 ± 0.165 mA, Fig. 4A). More overlapping threshold ranges implies higher number of probabilistically active MUs leading to a higher level of alternation. Fig. 4B shows the number of probabilistically active MUs after 1000 runs, which peaks at approximately 43 (33–52) (median, 5th–95th percentile).

Table 1
Threshold properties of individual motor units and stimulus currents required to elicit compound muscle action potential scans in fourteen healthy subjects for every stimulus duration.

Stimulus duration (ms)	Individual motor units			CMAP scans			
	μ (mA)	σ (mA)	RS ^a (%)	S5 (mA)	S50 (mA)	S95 (mA)	RR ^a (%)
0.1	9.8 ± 4.4	0.16 ± 0.10	1.5 ± 0.4	13.8 ± 5.4	17.1 ± 5.7	20.3 ± 6.5	39.1 ± 15.3
0.2	6.3 ± 2.7	0.11 ± 0.08	1.7 ± 0.4	8.5 ± 3.3	10.5 ± 3.6	12.5 ± 4.1	39.1 ± 15.0
0.6	3.8 ± 1.5	0.07 ± 0.04	1.7 ± 0.4	4.7 ± 1.8	5.9 ± 2.0	7.3 ± 2.4	45.1 ± 14.3
1.0	3.3 ± 1.3	0.06 ± 0.03	1.6 ± 0.5	3.9 ± 1.5	5.0 ± 1.7	6.3 ± 2.1	48.7 ± 12.0

μ = mean activation threshold of individual motor units, σ = standard deviation of the activation threshold of individual motor units, RS = relative spread; RR = relative range, CMAP = compound muscle action potential, S5 = target CMAP to elicit 5% of the maximum CMAP, S50 = target CMAP to elicit 50% of the maximum CMAP, S95 = target CMAP to elicit 95% of the maximum CMAP. Values are mean ± standard deviation.

^a Determined within every individual subject before averaging.

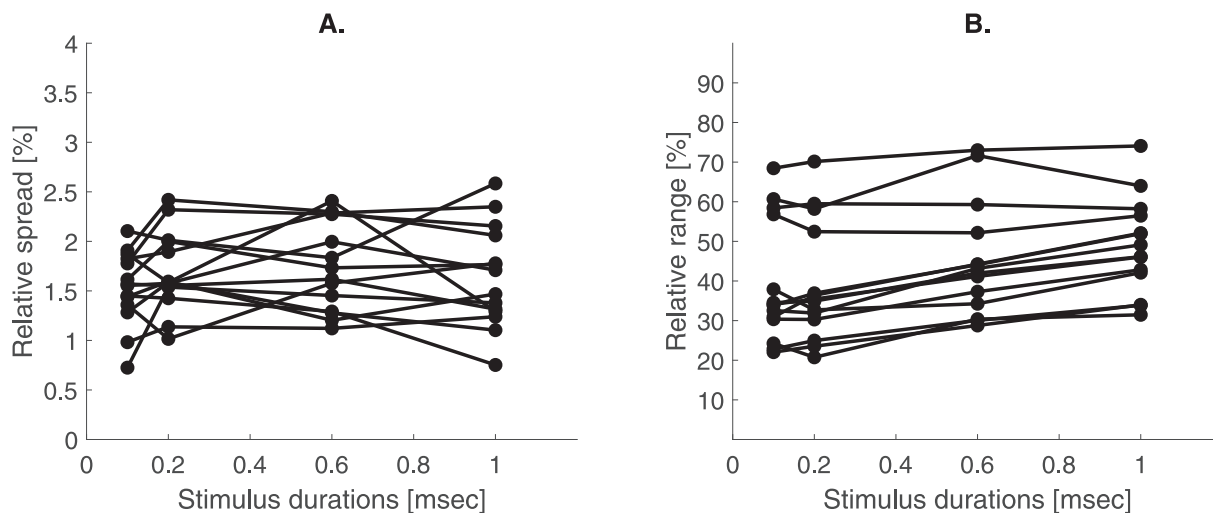


Fig. 2. Relation between stimulus duration, relative spread and range. (A) The relative spread in individual motor units (MUs) and (B) the relative range in compound muscle action potential scans expressing the distribution of MU activation thresholds determined within the fourteen healthy subjects at stimulus durations of 0.1, 0.2, 0.6 and 1.0 ms. Every line corresponds to an individual subject.

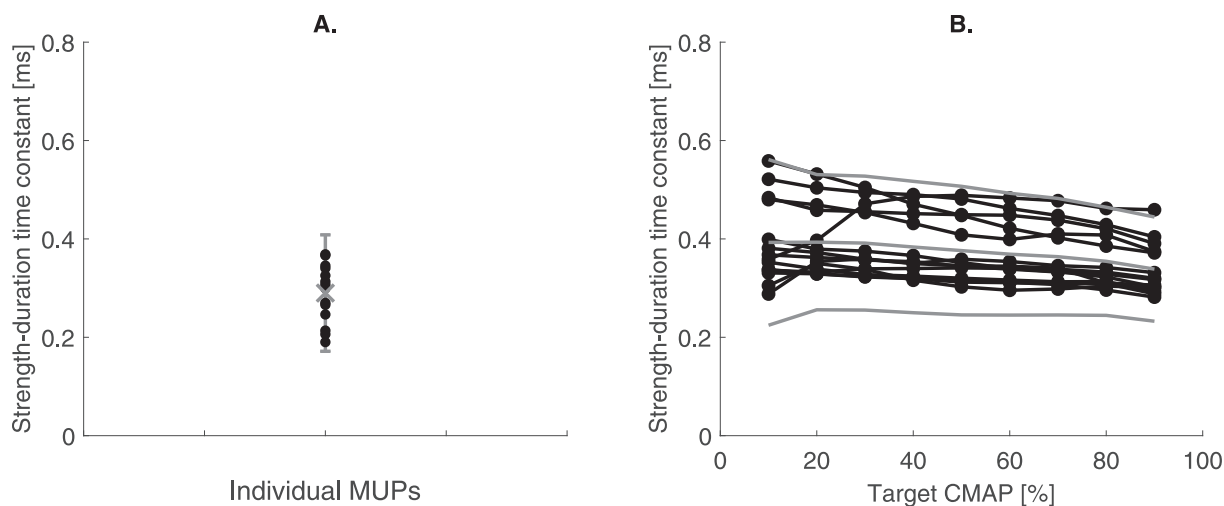


Fig. 3. Strength-duration time constant in individual motor units and at different target compound muscle action potentials. (A) The strength-duration time constants (SDTCs) in individual motor units (black dots) with mean ± 2 standard deviations (gray cross and error bar) and (B) the SDTC across target compound muscle action potentials from 10% to 90% obtained within the 14 healthy subjects. The gray lines represent the mean ± 2 standard deviations. SDTC = strength-duration time constant, CMAP = compound muscle action potential.

3.5. Impact of stimulus duration on the distribution of thresholds and alternation in CMAP scans

To determine the impact of stimulus duration on the distribution of MU activation thresholds within the CMAP scan, we

assigned a linearly decreasing SDTC in the simulations (from 0.40 to 0.34 ms, from low-to-high activation thresholds) at 1.0 ms (Fig. 5A, continuous). This resulted in a simulated mean of 17 mA for the activation thresholds at 0.1 ms (Fig. 5B, dashed), which corresponded well with our experiments at 0.1 ms (Table 1, S50). By

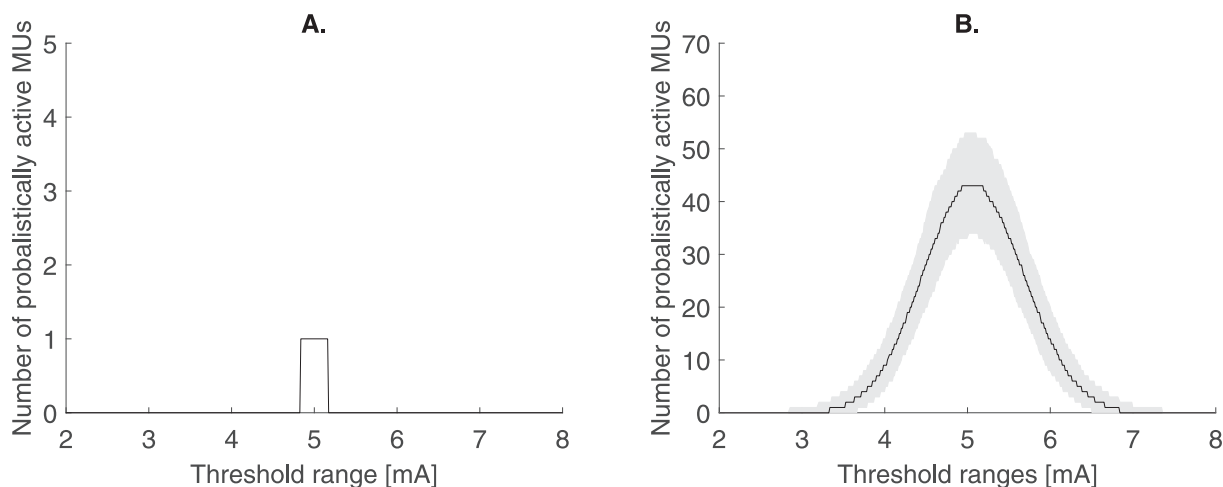


Fig. 4. Simulations on number of probabilistically active motor units across different threshold ranges. (A) Threshold range of one probabilistically active motor unit (MU) that defines the region of alternation (5.0 ± 0.165 mA with $RS = 1.65\%$). (B) Number of probabilistically active MUs for a fixed MU pool of 200 MUs after 1000 runs. The gray areas represent the 5th–95th percentile. MUs = motor units.

normalization, we also compared the relative distribution of thresholds between 1.0 ms and 0.1 ms. We found that a stimulus duration of 0.1 ms resulted in a higher peak (Fig. 5B, vertical arrow) with a relative narrower distribution compared to 1.0 ms (Fig. 5B, arrows 1 and 2). This means that for a CMAP scan generated with a stimulus duration of 0.1 ms relative more MUs are recruited in the middle (more alternation) and less MUs at its tails (less alternation).

Next, we plotted the measured set of relative thresholds over the entire CMAP scan for 0.1 ms against the set of relative thresholds for 1.0 ms for the fourteen recordings (Fig. 6A, black error bars). On top, we also plotted the simulated distribution of MU activation thresholds for 0.1 ms against 1.0 ms (Fig. 6A, gray squares) in individual runs ($n = 1000$). This showed a clear overlap between experiments and simulations, indicating that the linear trend in SDTC may underlie the smaller RR at 0.1 ms. As such, the stimulus duration significantly affects the level of alternation in CMAP scans, because the strength-duration properties are not identical for every MU. Fig. 6B shows an illustrative example, where a CMAP scan generated with 0.1 ms compared to 1.0 ms showed visible steps at the tails likely originating from a low number of alternating MUs.

4. Discussion

Our study examined the impact of stimulus durations involved in generating CMAP scans. Our results showed that the stimulus duration predominantly affected the distribution of MU activation thresholds, while the threshold variability of individual MUs remained constant. Our simulations also revealed that for a shorter stimulus duration, the level of alternation is higher (i.e. more probabilistically active MUs) in the middle part of the CMAP scan, while it was relatively reduced at its tails. Therefore, isolated MU responses will be easier detectable at the tails of the CMAP scan, especially when a shorter stimulus duration is applied. Consequently, under pathological conditions detection of enlarged MUs due to reinnervation with CMAP scans may be more sensitive with shorter stimulus durations, however one should remain vigilant that they need to be evaluated by their sizes. Similarly, deriving motor nerve dysfunction from the CMAP scan (Drenthen et al., 2013, 2014; van der Heyden et al., 2013) requires careful consideration of the impact of stimulus duration when defining reference values. Taken together, our results indicate the need for standard-

ization of applied stimulation settings of the CMAP scan to harmonize its use and facilitate interpretation of data from different studies.

4.1. Distribution of MU activation thresholds in the CMAP scan

Our data showed that the distribution of MU activation threshold flattened with longer stimulus durations, and found that this appeared to result from a subtle linearly decreasing trend of SDTC from low-to-high threshold MUs (i.e. low-to-high target CMAPs). The activation threshold and SDTC depend on a complex interplay of various factors (Bostock, 1983; Kuhn et al., 2009; Major and Jones, 2005; Mogyoros et al., 1996). Given that the experimental technique, applied stimulation electrodes, and nerve conditions in our healthy subjects remained the same in our study, the factors associated with this trend may be narrowed down to geometrical factors, such as axon depth and diameter. An axon at greater depth tends to prolong SDTC (Kuhn et al., 2009) at higher thresholds, whereas a larger axon diameter tends to prolong SDTC at lower thresholds. These two processes have opposing effects where simulations have suggested a stronger diameter-dependence of the activation threshold (Major and Jones, 2005), resulting in a net effect that may underlie the subtle linear trend observed for SDTC over the target CMAPs. This corroborates previous studies in which a longer SDTC at lower CMAPs could be observed (Kiernan et al., 2000; Mogyoros et al., 1996; Shibuta et al., 2010, 2013; Trevillion et al., 2010; Weerasinghe et al., 2017), although the marked variability between subjects may have masked a subtle linear relationship when assessed on group level (Kiernan et al., 2000; Mogyoros et al., 1996; Weerasinghe et al., 2017). Interestingly, presence of significance showed a consistent increased SDTC for the lower target CMAPs (Shibuta et al., 2010, 2013; Trevillion et al., 2010). It can be further observed in multiple nerve-muscle combinations (Bae et al., 2009). In the current study, we provided a comprehensive view by generating CMAP scans that automatically included all target levels from which we assessed SDTC within individual subjects. Moreover, we have verified the experimental observations with additional simulations. We assigned low-to-high threshold MUs a linear relationship of SDTC resulting in substantial overlap between the recorded set of relative thresholds and simulated relative distribution of MU activation thresholds (Fig. 6A). We do acknowledge that the simulated curves represent an average of many iterations, while in the experiments SDTC fluctuated consid-

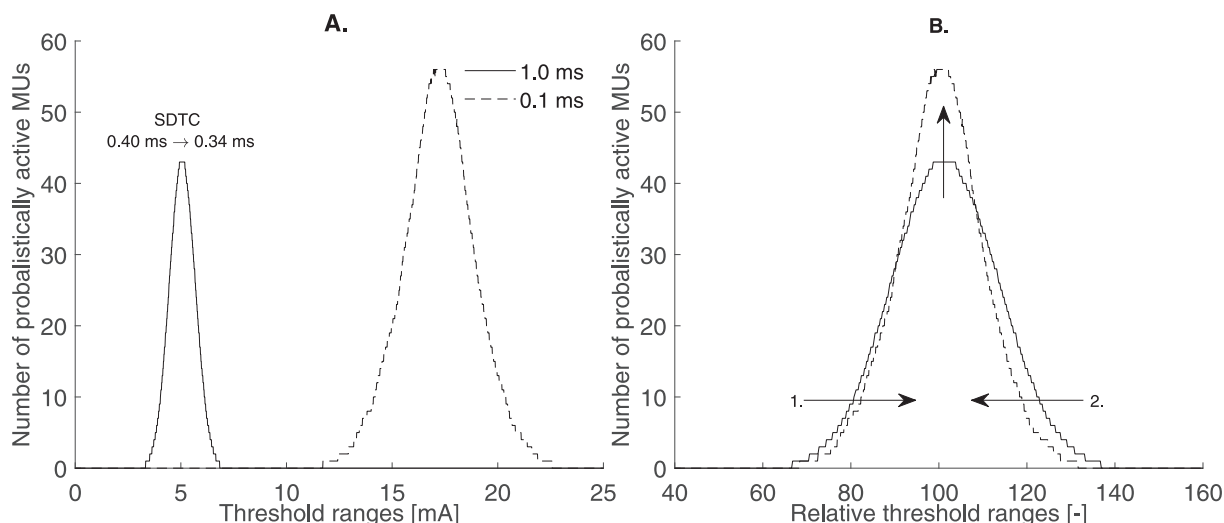


Fig. 5. Impact of stimulus duration on distribution of thresholds and alternation in compound muscle action potential scans (A) The simulated (continuous, 1.0 ms) and calculated (dashed, 0.1 ms) distribution of thresholds of a fixed set of 200 motor units (MUs) using a linear decreasing strength-duration time constant from 0.40 ms to 0.34 ms. (B) The relative distribution of thresholds at 1.0 ms (continuous) and 0.1 ms (dashed) showed for 0.1 ms a higher peak in the middle (i.e. more alternation, vertical arrow) and smaller number of probabilistically active MUs at its tails (i.e. less alternation, arrows 1 and 2). MUs = motor units, SDTC = strength-duration time constant.

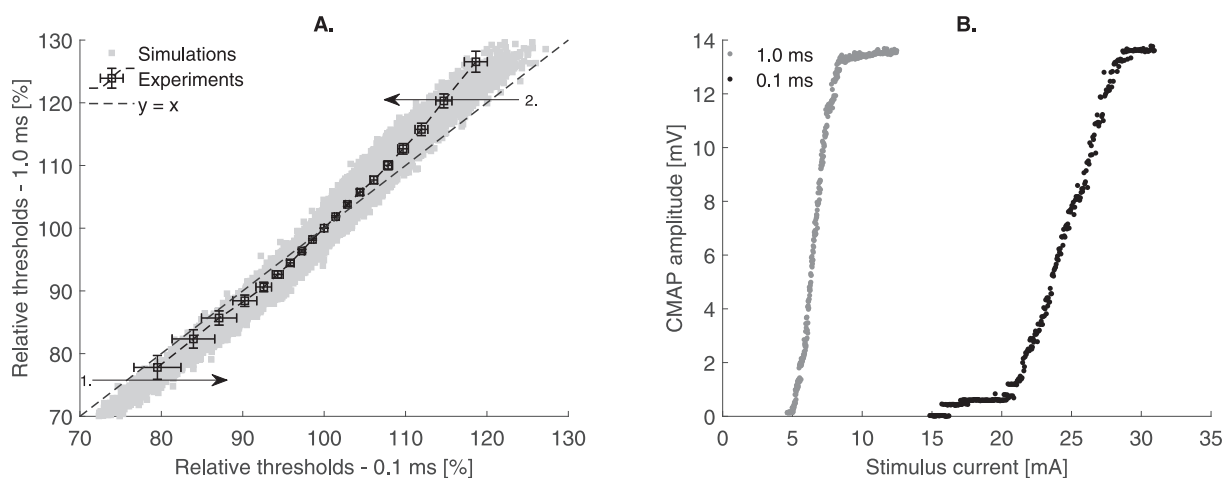


Fig. 6. Comparison of the set of relative thresholds from experiments and relative threshold ranges from simulations. (A) The set of relative thresholds at 0.1 ms plotted against at 1.0 ms for the 14 recordings (black error bars, mean ± standard error of the mean) and simulated relative threshold ranges (gray squares – 1000 runs). Arrows 1 and 2 present the narrower range of relative thresholds in which all MUs are activated similar to arrows 1 and 2 in Fig. 5B. Line of unity (black dashed) (B) Illustrative example of two compound muscle action potential (CMAP) scans at 1.0 and 0.1 ms within a single subject with the emergence of steps in the CMAP scan generated by a 0.1 ms stimulus duration due to the low level of alternation at the tails of the CMAP scan. CMAP = compound muscle action potential.

erably across target CMAPs. Additionally, SDTC of individual MUs are likely to harbour more variability, because SDTC at target CMAPs represent an average from a group of motor axons. In practice, careful isolation of individual MUP responses may result in activating more superficial axons, which may shift the net effect towards a more depth dependence. These two factors may explain the counterintuitive smaller SDTC in individual MUs compared to SDTC at target CMAPs (Mogyoros et al., 1996). Taken together, the degree of the linear relationship should be interpreted with caution in individual cases, especially under pathological conditions where it may be masked by increased variability of SDTC (Shibuta et al., 2013) or under conditions with marked loss of MUs.

4.2. Threshold variability of individual MUs in the CMAP scan

Our study confirmed that the stimulus duration had no effect on the threshold variability quantified by RS within individual MUs in human subjects. Although, we have studied a relative small range

(0.1–1.0 ms), the independence of RS to stimulus duration agrees with previous studies, which were limited to animal and computer models (Lecar and Nossal, 1971a,b; Verveen, 1960). The averaged RS of 1.65% in our study matched well with other experiments in human subjects (Hales et al., 2004). Such a similar finding observed in an independent healthy cohort provides highly relevant insights on the physiological window within which MUs operate. A constant RS indicates a broader absolute threshold variability for high-threshold MUs compared to low-threshold MUs. Consequently, to sample the RS equally across the a priori unknown distribution of MU activation thresholds within the CMAP scan requires stimuli applied with an exponential decrease in stimulus currents (Bostock, 2016). Additionally, RS and SDTC have been suggested to be associated with nodal persistent sodium channels (Bostock and Rothwell, 1997; Hales et al., 2004; Mogyoros et al., 1998). In the current study we did not find a relation between RS and SDTC within individual MUs, which may be due the marked variability of RS between stimulus durations.

4.3. Alternation and implications for MU number estimation and appearance of steps

To obtain a reliable and reproducible MU number estimate, one of the challenging aspects involve alternation. Due to threshold variability the range in which MUs show their typical alternating (all-or-none) behaviour may overlap. As a result, the number of MUs with overlapping thresholds induce an exponentially increasing number of possible combinations, which far exceeds the number of samples applied within the CMAP scan (Sleutjes et al., 2014). This emphasizes the need to make optimal use of the recording and stimulation settings. Due to the impact of stimulus duration on alternation within the CMAP scan, the slope and variance of the CMAP scan alters, which consequently affects MU estimates derived from the CMAP scan (Zong et al., 2020). We established that a short compared to long stimulus duration further lowered the number of alternating MUs at the tails of the CMAP scan (Fig. 5). A short stimulus duration is therefore preferred for MUNE methods that require collecting a sample of low-threshold MUs. Due to the lower number of alternating MUs at the tails, the appearance of steps (Fig. 6B) are not uncommon at the bottom and top of CMAP scans in healthy subjects (Blok et al., 2007; Henderson et al., 2006; Maathuis et al., 2011). As this study shows, the likelihood of these steps at the tails increases when applying a short stimulus duration (e.g. 0.1 ms) to generate CMAP scans. Steps or discontinuities that start to appear in the middle part of the CMAP scan or when their amplitude contribute substantially relative to the maximum CMAP (Sleutjes et al., 2014) raises the likelihood of a pathological origin. Additionally, given the fact that depolarizing the membrane potential to generate an action potential is more accurately defined with a shorter stimulus duration, it may also induce less temporal dispersion. Less temporal dispersion may also be favourable as most MUNE methods assume that individual MUPs have an additive contribution to produce the CMAP.

4.4. Experimental and model limitations

Our study has several limitations. For simulating alternation, we assumed a uniform probability over the threshold range, while the probabilistic function for individual MUs follows a cumulative Gaussian distribution (Hales et al., 2004). To further simplify the simulations, we used an additive approach of the threshold ranges, without simulating the true probabilistic nature of MUs. Furthermore, we assumed a symmetric normal distribution of MU activation thresholds, although this may not be the case for CMAP scans. However, our study was not directly aimed at the absolute number of alternating MUs and type of distribution, but rather at evaluating the potential changes to the distribution induced by the stimulus duration. As both a smaller or larger MU pool would induce similar changes to the distribution, we preferred a fixed number of MUs as this also facilitated comparison between experimental data and simulations. The large error bars of the level of alternation (Fig. 4B) may partly express the variability in CMAP scans that we encountered between individual subjects. To overcome the assumption of symmetric MU activation thresholds within the CMAP scan, we defined a set of relative thresholds. Despite that we disregarded variability in MU sizes for practical reasons, our simulations on changes in the distribution of thresholds were in good agreement with our experiments on the changes in relative thresholds. It is expected that more realistic distributions of MU sizes (Ridall et al., 2007) may further improve the simulations. As we have only investigated one individual low-threshold MU per subject, we could not directly determine whether low-to-high threshold MUs had differences in RS. Nevertheless, we found no relation between RS and stimulus currents for the set of applied stimulus durations.

5. Conclusion

Stimulation settings of the CMAP scan require further standardization as stimulus duration can affect the electrical recruitment of MUs illustrated by our experiments and computer simulations. Our data shows that a shorter stimulus duration may be preferred, as steps or discontinuities and importantly, their sizes, can be easier evaluated due to the increased likelihood of their appearance at the tails of the CMAP scan. This could improve early detection of enlarged MUs under pathological conditions. However, this may also reduce its specificity. Therefore, the presence of steps or discontinuities at the tails should be carefully judged by their sizes. Mitigating alternation may also provide an important opportunity to improve existing MUNE methodologies. The fact that the stimulus duration already had a detectable influence on alternation in our study, illustrates the possibilities to further optimize the recording and stimulation settings. Taken together, our study emphasizes the importance to provide details on the applied stimulation settings in studies that use CMAP scans. Standardization of these settings is preferred when using different EMG platforms and during successive visits in its use for monitoring of the disease progression.

Declaration of Competing Interest

The authors declare that they have no known competing financial interests or personal relationships that could have appeared to influence the work reported in this paper.

Acknowledgement

This study was supported by the Netherlands ALS foundation (Stichting ALS Nederland).

References

- Aggarwal A. Handgrip maximal voluntary isometric contraction does not correlate with thenar motor unit number estimation. *Neurol Res Int* 2012;2012:187947.
- Bae JS, Sawai S, Misawa S, Kanai K, Iose S, Kuwabara S. Differences in excitability properties of FDI and ADM motor axons. *Muscle Nerve* 2009;39:350–4.
- Baumann F, Henderson RD, Gareth Ridall P, Pettitt AN, McCombe PA. Quantitative studies of lower motor neuron degeneration in amyotrophic lateral sclerosis: evidence for exponential decay of motor unit numbers and greatest rate of loss at the site of onset. *Clin Neurophysiol* 2012a;123:2092–8.
- Baumann F, Henderson RD, Ridall PG, Pettitt AN, McCombe PA. Use of Bayesian MUNE to show differing rate of loss of motor units in subgroups of ALS. *Clin Neurophysiol* 2012b;123:2446–53.
- Blok JH, Ruitenbergh A, Maathuis EM, Visser GH. The electrophysiological muscle scan. *Muscle Nerve* 2007;36:436–46.
- Bostock H. The strength-duration relationship for excitation of myelinated nerve: computed dependence on membrane parameters. *J Physiol* 1983;341:59–74.
- Bostock H. Estimating motor unit numbers from a CMAP scan. *Muscle Nerve* 2016;53:889–96.
- Bostock H, Rothwell JC. Latent addition in motor and sensory fibres of human peripheral nerve. *J Physiol* 1997;498:277–94.
- de Carvalho M, Barkhaus PE, Nandedkar SD, Swash M. Motor unit number estimation (MUNE): Where are we now?. *Clin Neurophysiol* 2018;129:1507–16.
- Drenthen J, Maathuis EM, Ruts L, van Doorn PA, Blok JH, Visser H. Serial CMAP scan analysis in Guillain-Barre patients. *J Peripher Nerv Syst* 2008;13.
- Drenthen J, Maathuis EM, Visser GH, van Doorn PA, Blok JH, Jacobs BC. Limb motor nerve dysfunction in Miller Fisher syndrome. *J Peripher Nerv Syst* 2013;18:25–9.
- Drenthen J, Roodbol J, Maathuis EM, Catsman-Berrevuets CE, van Doorn PA, Blok JH, et al. Motor nerve excitability after childhood guillain-barre syndrome. *J Peripher Nerv Syst* 2014;19.
- Garg N, Howells J, Yiannikas C, Vucic S, Krishnan AV, Spies J, et al. Motor unit remodelling in multifocal motor neuropathy: The importance of axonal loss. *Clin Neurophysiol* 2017;128:2022–8.
- Gejo-Barrientos E, Pastore-Olmedo C, De Mingo P, Blanquer M, Gomez Espuch J, Iniesta F, et al. Intramuscular injection of bone marrow stem cells in amyotrophic lateral sclerosis patients: A randomized clinical trial. *Front Neurosci* 2020;14:195.

- Gooch CL, Doherty TJ, Chan KM, Bromberg MB, Lewis RA, Stashuk DW, et al. Motor unit number estimation: a technology and literature review. *Muscle Nerve* 2014;50:884–93.
- Hales JP, Lin CS, Bostock H. Variations in excitability of single human motor axons, related to stochastic properties of nodal sodium channels. *J Physiol* 2004;559:953–64.
- Henderson RD, Ridall GR, Pettitt AN, McCombe PA, Daube JR. The stimulus-response curve and motor unit variability in normal subjects and subjects with amyotrophic lateral sclerosis. *Muscle Nerve* 2006;34:34–43.
- Henderson RD, Ridall PG, Hutchinson NM, Pettitt AN, McCombe PA. Bayesian statistical MUNE method. *Muscle Nerve* 2007;36:206–13.
- Henderson RD, Ridall PG, Pettitt AN, McCombe PA. Results of Bayesian statistical analysis in normal and ALS subjects. *Suppl Clin Neurophysiol* 2009;60:57–63.
- Jacobsen AB, Bostock H, Fuglsang-Frederiksen A, Duez L, Beniczky S, Moller AT, et al. Reproducibility, and sensitivity to motor unit loss in amyotrophic lateral sclerosis, of a novel MUNE method: MScanFit MUNE. *Clin Neurophysiol* 2017;128:1380–8.
- Jacobsen AB, Bostock H, Tankisi H. Following disease progression in motor neuron disorders with 3 motor unit number estimation methods. *Muscle Nerve* 2019;59:82–7.
- Kiernan MC, Burke D, Andersen KV, Bostock H. Multiple measures of axonal excitability: a new approach in clinical testing. *Muscle Nerve* 2000;23:399–409.
- Kuhn A, Keller T, Lawrence M, Morari M. A model for transcutaneous current stimulation: simulations and experiments. *Med Biol Eng Comput* 2009;47:279–89.
- Lecar H, Nossal R. Theory of threshold fluctuations in nerves. II. Analysis of various sources of membrane noise. *Biophys J* 1971a;11:1068–84.
- Lecar H, Nossal R. Theory of threshold fluctuations in nerves. I. Relationships between electrical noise and fluctuations in axon firing. *Biophys J* 1971b;11:1048–67.
- Maathuis EM, Drenthen J, van Doorn PA, Visser GH, Blok JH. The CMAP scan as a tool to monitor disease progression in ALS and PMA. *Amyotroph Lateral Scler Frontotemporal Degener* 2013;14:217–23.
- Maathuis EM, Drenthen J, Visser GH, Blok JH. Reproducibility of the CMAP scan. *J Electromyogr Kinesiol* 2011;21:433–7.
- Maathuis EM, Henderson RD, Drenthen J, Hutchinson NM, Daube JR, Blok JH, et al. Optimal stimulation settings for CMAP scan registrations. *J Brachial Plex Peripher Nerve Inj* 2012;7:4.
- Major LA, Jones KE. Simulations of motor unit number estimation techniques. *J Neural Eng* 2005;2:17–34.
- McComas AJ, Fawcett PR, Campbell MJ, Sica RE. Electrophysiological estimation of the number of motor units within a human muscle. *J Neurol Neurosurg Psychiatry* 1971;34:121–31.
- Milner-Brown HS, Brown WF. New methods of estimating the number of motor units in a muscle. *J Neurol Neurosurg Psychiatry* 1976;39:258–65.
- Mogyoros I, Kiernan MC, Burke D. Strength-duration properties of human peripheral nerve. *Brain* 1996;119:439–47.
- Mogyoros I, Kiernan MC, Burke D, Bostock H. Strength-duration properties of sensory and motor axons in amyotrophic lateral sclerosis. *Brain* 1998;121:851–9.
- Ridall PG, Pettitt AN, Friel N, McCombe PA, Henderson RD. Motor unit number estimation using reversible jump Markov chain Monte Carlo methods. *J R Stat Soc C-Appl* 2007;56:235–60.
- Shibuta Y, Nodera H, Mori A, Okita T, Kaji R. Peripheral nerve excitability measures at different target levels: the effects of aging and diabetic neuropathy. *J Clin Neurophysiol* 2010;27:350–7.
- Shibuta Y, Shimatani Y, Nodera H, Izumi Y, Kaji R. Increased variability of axonal excitability in amyotrophic lateral sclerosis. *Clin Neurophysiol* 2013;124:2046–53.
- Sleutjes BTHM, Drenthen J, Boskovic E, van Schelven LJ, Kovalchuk MO, Lumens PGE, et al. Excitability tests using high-density surface-EMG: A novel approach to studying single motor units. *Clin Neurophysiol* 2018;129:1634–41.
- Sleutjes BTHM, Montfoort I, Maathuis EM, Drenthen J, van Doorn PA, Visser GH, et al. CMAP scan discontinuities: automated detection and relation to motor unit loss. *Clin Neurophysiol* 2014;125:388–95.
- Sleutjes BTHM, Wijngaarde CA, Wadman RI, Otto LAM, Asselman FL, Cuppen I, et al. Assessment of motor unit loss in patients with spinal muscular atrophy. *Clin Neurophysiol* 2020;131:1280–6.
- Trevillion L, Howells J, Bostock H, Burke D. Properties of low-threshold motor axons in the human median nerve. *J Physiol* 2010;588:2503–15.
- van der Heyden J, van der Meer P, Birnie E, de Coo IF, Castro Cabezas M, Ozcan B, et al. Decreased excitability of the distal motor nerve of young patients with type 1 diabetes mellitus. *Pediatr Diabetes* 2013;14:519–25.
- Verveen AA. In: On the Fluctuation of Threshold of the Nerve Fibre. Structure and function of the cerebral cortex. Amsterdam: Elsevier; 1960. p. 282–8.
- Weerasinghe D, Menon P, Vucic S. Hyperpolarization-activated cyclic-nucleotide-gated channels potentially modulate axonal excitability at different thresholds. *J Neurophysiol* 2017;118:3044–50.
- Zong Y, Lu Z, Zhang L, Li X, Zhou P. Motor unit number of the first dorsal interosseous muscle estimated from CMAP scan with different pulse widths and steps. *J Neural Eng* 2020;17:014001.